Journal of Materials Science and Chemical Engineering, 2023, 11, 20-30
https://www.scirp.org/journal/msce
ISSN Online: 2327-6053
ISSN Print: 2327-6045

Structural, Optical and Photocatalytic Properties of Cu^{2+} Doped ZnO Nanorods with Using HMTA Solvent Prepared by Hydrothermal Method

Nguyen Thi Tuyet Mai*, Nguyen Thi Lan, Trinh Xuan Anh, Ta Ngoc Dung, Huynh Dang Chinh

School of Chemical Engineering, Hanoi University of Science and Technology, Hanoi, Vietnam
Email: *mai.nguyenthituyet@hust.edu.vn

How to cite this paper: Mai, N.T.T., Lan, N.T., Anh, T.X., Dung, T.N. and Chinh, H.D. (2023) Structural, Optical and Photocatalytic Properties of Cu^{2+} Doped ZnO Nanorods with Using HMTA Solvent Prepared by Hydrothermal Method. *Journal of Materials Science and Chemical Engineering*, **11**, 20-30.
https://doi.org/10.4236/msce.2023.117003

Received: May 23, 2023
Accepted: July 16, 2023
Published: July 19, 2023

Abstract

In this experiment, Cu^{2+} doped ZnO (Cu-ZnO) nanorods materials have been fabricated by hydrothermal method. Cu^{2+} ions were doped into ZnO with ratios of 2, 5 and 7 mol.% (compared to the mole's number of Zn^{2+}). The hexamethylenetetramine (HMTA) solvent used for the fabrication of Cu-ZnO nanorods with the mole ratio of Zn^{2+}:HMTA = 1:4. The characteristics of the materials were analyzed by techniques, such as XRD, Raman shift, SEM and UV-vis diffuse reflectance spectra (DRS). The photocatalytic properties of the materials were investigated by the decomposition of the methylene blue (MB) dye solution under ultraviolet light. The results show that the size of Cu-ZnO nanorods was reduced when the Cu^{2+} doping ratio increased from 2 mol.% to 7 mol.%. The decomposition efficiency of the MB dye solution reached 92% - 97%, corresponding to the Cu^{2+} doping ratio changed from 2 - 7 mol.% (after 40 minutes of ultraviolet irradiation). The highest efficiency for the decomposition of the MB solution was obtained at a Cu^{2+} doping ratio of 2 mol.%.

Keywords

Cu^{2+} Doped ZnO Nanorods, ZnO Nanomaterials, Hexamethylenetetramine (HMTA), Photocatalytics, Methylene Blue, Hydrothermal Method, UV Irradiation

1. Introduction

Research semiconductor is one of the important research activities being carried out around the world. Potential application areas are diverse due to the unique and interesting properties of semiconductor materials, such as optoelectron-

ics, photonics, laser diodes, sensors, polymer-based flexible solar cells, color-sensitive solar battery electrodes, etc. [1] [2] [3] [4]. In particular, ZnO semiconductor is one of the potential candidates to be studied for the above application fields due to its wide gap width (3.37 eV) and large exciton energy (60 meV) at temperature room [5]-[12]. Recently, white light emitting diode material (LED) based on ZnO nanostructure as an alternative source for energy-saving light sources has been developed and studied by many research groups [13]-[17]. In addition, ZnO is the most abundant nanostructured material, such as nanowires, nanofibers, nanorods, pyramids, spheres, flowers, etc., so ZnO nanomaterials (ZnO NMs) are being studied the most to improve the properties of the applied materials [18]-[26]. Currently, the using of ZnO nanomaterials doped with transition metal ions on an industrial scale is continuously encouraging researchers to change and improve physical, chemical, and electrical properties, etc., so that it becomes a better material for many applications [27]-[35]. ZnO NMs have been synthesized by various methods, such as wet chemical method, solution combustion, sol-gel synthesis, chemical precipitation, solvothermal/hydrothermal reaction, etc. [10] [19]-[27] [29] [33] [35]. Some of these fabrication methods have limitations, for example, it is difficult to control the growth of the nanostructure of the fabricated materials due to the reaction rate or reaction temperature in the sol-gel reactions, chemical precipitation, solution combustion, etc. Among the above methods, the hydrothermal fabrication method is considered a promising advantage method because this method is simple, the simple equipment, the synthesis at low temperature, easy to control the grain size, large-scale uniform fabrication and environmental friendliness [19] [21] [23] [35].

In this work, we studied the fabrication of Cu^{2+} doped ZnO nanorods materials using hexamethylenetetramine solvent (with the ratio of Zn^{2+}:HMTA = 1:4) by hydrothermal method and investigated the photocatalytic properties for decomposition of methylene blue dye solution under ultraviolet irradiation.

2. Materials and Methods

2.1. Materials

All chemicals were of analytical grade and used without any further purification, including: Copper(II) nitrate trihydrate ($Cu(NO_3)_2{\cdot}3H_2O$, 99.8%, AR-China); Zinc nitrate hexahydrate ($Zn(NO_3)_2{\cdot}6H_2O$, 98%, AR-China); Hexamethylenetetramine (HMTA, $C_6H_{12}N_4$, 95%, AR-China). All solutions were prepared with double distilled water.

2.2. Sample Synthesis

A mixed solution of 0.1 M $Zn(NO_3)_2$ and 0.1 M HMTA was uniformly mixed in a volume ratio of 1:4 on a magnetic stirrer at constant speed for 15 minutes. To doped Cu^{2+} into the above-mixed solution, a solution of $Cu(NO_3)_2$ in the molar ratio of 0, 2%, 5% and 7% (calculated compared to the number of moles of Zn^{2+}) was slowly added to the mixed solution. The mixed solution was continuously

stirred for another 5 minutes and then transferred to a 100 mL Teflon to carry out the hydrothermal reaction at 90˚C for 6 hours. The precipitate obtained after hydrothermal process was filtered and washed several times with double distilled water until the pH ≈ 7. Next, the clean precipitate was dried at 80˚C for 24 hours. The final product was a fine white or blue powder depending on the doped Cu ion content. Synthetic powder product samples were denoted as pure ZnO, 2%Cu-ZnO, 5%Cu-ZnO and 7%Cu-ZnO samples with Cu^{2+} doped content of 0, 2, 5 and 7 mol.% (compared to the mole's number of Zn^{2+}), respectively. Figure 1 showed images of pure ZnO, 2%Cu-ZnO, 5%Cu-ZnO and 7%Cu-ZnO samples after hydrothermal process were filtered and washed and preparation for the next step was to dry at 80˚C for 24 hours to obtain the Cu^{2+} doped ZnO samples, respectively.

2.3. Characterization

X-ray diffraction (XRD) patterns were measured on a X'pert Pro (PANalytical) MPD using Cu-K_α radiation (λ = 1.54065 Å, scan speed: 0.03˚/2s, $2\theta \approx 25^\circ$ - 75˚). Raman shift spectra were measured on MicroRaman LABRAM-1B (laser wavelength: 633 nm, laser power: 6.25 mW, Leica NPLAN L50x/0.50 BD microscope). Scanning electron microscopy/X-ray energy scattering spectra (SEM/EDX) were measured on a HITACHI TM4000 Plus. Reflectance spectra were measured on a Jasco V-750, DRUV-Vis (using a 60 mm integrated sphere of ISV-922, scan speed: 200 nm/min). Liquid UV-Vis absorption spectra were measured on an Agilent 8453.

2.4. Photocatalysis

The photocatalytic activity of the prepared samples was evaluated by degradation the methylene blue (MB) solution. 50 mg of the nanopowder catalyst was suspended in a pyrex containing 60 mL of 10 ppm methylene blue aqueous solution. Then, the mixture was stirred for 60 min in dark to obtain the adsorption-desorption equilibrium. The reaction mixture was exposed to ultraviolet light by a SH-HB2-200W Highbay lamp with central wavelength emission at 370 nm. After every 10 minutes of irradation, 5 ml of the solution was taken out, filtered, centrifuged to get the solution that had separated the catalyst powder and measured the absorbance of those selected solution on a UV-vis spectrophotometer (VARRIAN Carry100) at the maximum wavelength of MB solution (λ = 660 nm). MB degradation was determined according to the formula below.

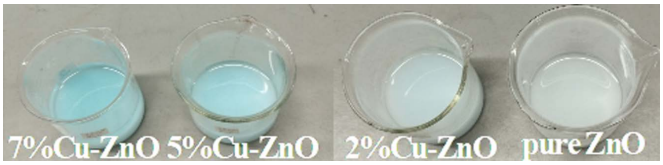

Figure 1. Images of pure ZnO, 2%Cu-ZnO, 5%Cu-ZnO and 7%Cu-ZnO samples after hydrothermal process were filtered and washed and preparation for the next step was to dry at 80˚C for 24 hours to obtain the Cu^{2+} doped ZnO samples, respectively.

$$D(\%) = \frac{C_0 - C}{C_0} \times 100 \quad (1)$$

where $D(\%)$ is the degradation of MB, %; C_0 is the initial concentration of MB (mM) ($t = 0$); C is the concentration of MB (mM) at time t (minutes).

3. Results and Discussion

3.1. Structural Properties

Define X-ray diffraction (XRD) patterns of pure ZnO, 2%Cu-ZnO, 5%Cu-ZnO and 7%Cu-ZnO samples are shown in Figure 2. On the XRD diagram, Figure 2 showed that the material samples all appear spectral peaks at 2θ diffraction angle positions of 31.7˚, 34.4˚, 36.3˚, 47.5˚, 56.6˚, 62.9˚, 67.9˚ and 69.1˚ correspond to the (100), (002), (101), (102), (110), (103), (112) and (201) lattice planes of the hexagonal wurtzite ZnO with space group (P63mc) (JCPDS card No. 89-7102) [18] [20] [28].

Diffraction spectra showed that all samples were in single phase and there were no anomalous peaks related to Cu metal clusters or Cu oxides secondary phases. This showed that the Cu ions doped ZnO samples retain the hexagonal wurtzite structure of ZnO. Also, it was attributed to the good dispersion of Cu^{2+} into the ZnO lattice [17] [20] [28] [29]. This can be explained that Cu has been doped into the ZnO lattice and Cu^{2+} ions have replaced Zn^{2+} ions because the atomic radii of these two ions are nearly equal ($r_{Zn^{2+}}$ = 0.074 nm and $r_{Cu^{2+}}$ = 0.072 nm) [17] [29]. The crystalline size of samples was calculated using the Scherrer formula [20] [28]:

$$d = \frac{0.89\lambda}{\cos\theta} \quad (2)$$

where d is the crystalline size (nm); λ is the wavelength of X-ray radiation (λ =

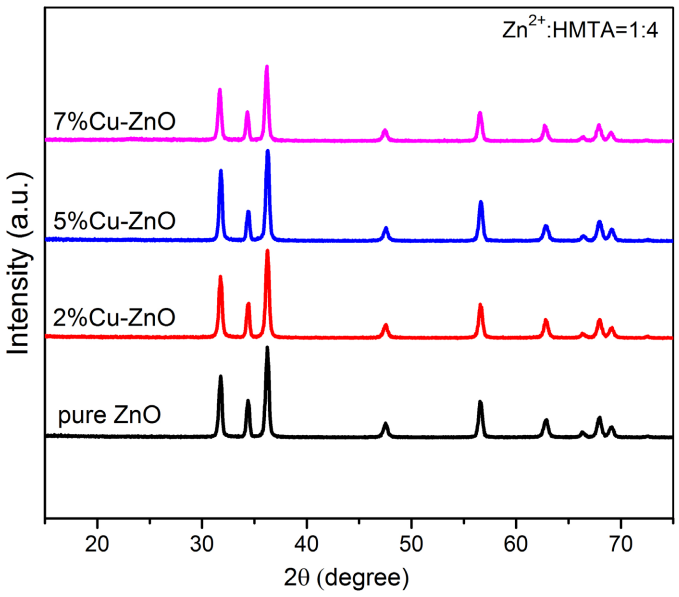

Figure 2. XRD patterns of pure ZnO, 2%Cu-ZnO, 5%Cu-ZnO and 7%Cu-ZnO samples.

1.54065 Å); θ is the Bragg angle (radians); β is full width half maxima (FWHM) of (101) diffraction peak (radians). The calculated crystallite size of pure ZnO, 2%Cu-ZnO, 5%Cu-ZnO and 7%Cu-ZnO samples were about 64.5 nm, 22.6 nm, 21.8 nm and 20.4 nm, respectively. This can be observed that the crystallite size of samples decreases from 64.5 nm to 20.4 nm when Cu^{2+} content increases from 0 mol.% to 7 mol.%, indicating that the Cu dopant inhibited the crystallization of ZnO samples.

The general chemical equation of the Cu^{2+} doped ZnO synthesis reaction could be described by the following mechanism [15] [19] [21]:

$$Zn(NO_3)_2 \xleftrightarrow{H_2O} Zn^{2+} + 2NO_3^- \quad (3)$$

$$C_6H_{12}N_4 + 6H_2O \xleftrightarrow{H_2O} 4NH_3 + 4HCOOH \quad (4)$$

$$NH_3 + H_2O \xleftrightarrow{H_2O} NH_4^+ + OH^- \quad (5)$$

$$Zn^{2+} + 2OH^- \xleftrightarrow{H_2O} Zn(OH)_2 \downarrow \quad (6)$$

$$Zn(OH)_2 \downarrow \xleftrightarrow[\text{Method}]{\text{Hydrothermal}} ZnO \downarrow + H_2O \quad (7)$$

$$Zn(NO_3)_2 + Cu(NO_3)_2 \xleftrightarrow[\text{Hydrothermal method}]{\text{HMTA}} Zn_{1-x}Cu_xO + \text{gaseous products} \quad (8)$$

3.2. Raman Spectra Analysis

Figure 3 showed the Raman spectra of pure ZnO, 2%Cu-ZnO, 5%Cu-ZnO and 7%Cu-ZnO samples. The Raman spectra showed that the fabricated samples all had Raman wave vibration positions corresponding to the wave vibration positions of the hexagonal wurtzite structure ZnO with space group P63mc [13] [18]. The peaks that were observed at 335 cm^{-1} and 390 cm^{-1} were assigned to the $E_{2(high)} - E_{2(low)}$ and $A_{1(TO)}$ modes of the hexagonal wurrtzite ZnO, respectively. The peak at 440 cm^{-1} was assigned to the $E_{1(TO)}$ mode of the hexagonal wurrtzite

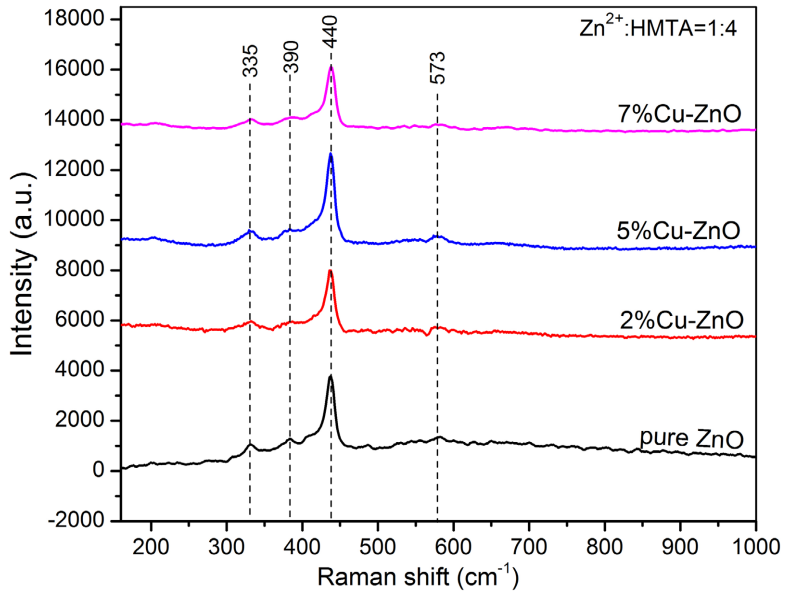

Figure 3. Raman spectra of pure ZnO, 2%Cu-ZnO, 5%Cu-ZnO and 7%Cu-ZnO samples.

ZnO. The peak at 573 cm^{-1} was assigned to the $E_{1(LO)}$ mode of the hexagonal wurrtzite ZnO [13] [18].

It could be seen that the wave vibration positions as wel as wave intensity of Raman spectra of the samples were almost similar, with no significant difference. It is possible that the doping amount of Cu^{2+} in the ZnO sample is small (≤7 mol.%). In addition, in the Raman spectra of pure ZnO and doped ZnO samples, there were no wave peaks corresponding to the vibration modes of CuO, Cu_2O or Cu. This could be explained similarly to above because the amount of Cu^{2+} doped into the lattice cell of ZnO is small (≤7 mol.%).

3.3. Morphological Characteristic

SEM images with different magnifications of pure ZnO, 2%Cu-ZnO, 5%Cu-ZnO and 7%Cu-ZnO samples were shown in **Figure 4**. The SEM images showed that the pure ZnO sample exhibit a nanorod structure with the thickness size of about 250 - 300 nm. The 2%Cu-ZnO sample exhibited a nanorods structure with the smaler thickness size (of about 20 - 30 nm). The 5%Cu-ZnO and 7%Cu-ZnO samples exhibited a tube structure in the meniscus form at the ends of the tube like a porosity meniscus tube with the thickness size of about 100 - 200 nm. Thus, it could be seen that when the content of doped Cu^{2+} in the ZnO lattice increased: it had the effect of preventing the growth of crystal grains. The crystals of the material samples grew in the form of rods with decreasing crystal size and increasing porosity.

3.4. Optical Properties

Figure 5 showed the plot between absorbance and wavelength for the pure ZnO,

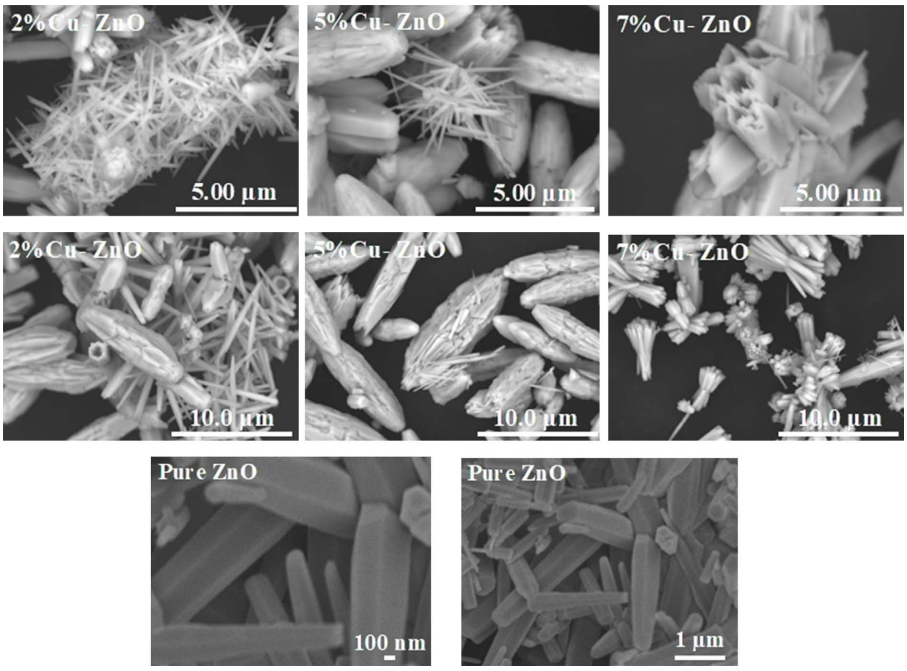

Figure 4. SEM images of the pure ZnO, 2%Cu-ZnO, 5%Cu-ZnO and 7%Cu-ZnO samples.

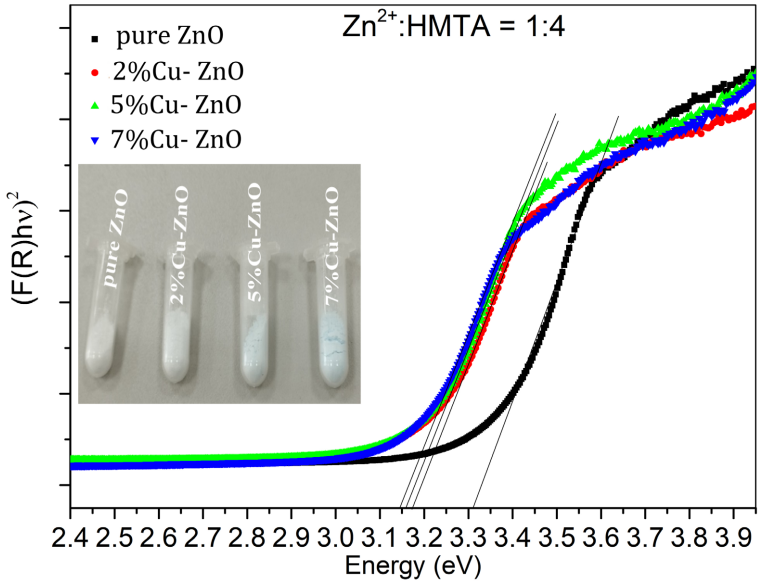

Figure 5. The plot between $(F(R)h\nu)^2$ and $h\nu$ based on K-M model of pure ZnO, 2%Cu-ZnO, 5%Cu-ZnO and 7%Cu-ZnO samples. Inset: Photographs of pure ZnO, 2%Cu-ZnO, 5%Cu-ZnO and 7%Cu-ZnO samples of the experiment.

2%Cu-ZnO, 5%Cu-ZnO and 7%Cu-ZnO samples. The inset showed the photographs of the prepared pure ZnO, 2%Cu-ZnO, 5%Cu-ZnO and 7%Cu-ZnO samples of the experiment. The Kubelka-Munk (K-M) model was used to determine the band gap of the prepared samples based on equation below:

$$F(R) = \frac{(1-R)^2}{2R} \tag{9}$$

where $F(R)$ was K-M function and R was reflectance [18] [20]. The band gap was found to be 3.31 eV, 3.17 eV, 3.16 eV and 3.15 eV for the pure ZnO, 2%Cu-ZnO, 5%Cu-ZnO and 7%Cu-ZnO samples, respectively. Here, it could be seen the band gap decreased gradually as the doping copper content increased gradually into the lattice of ZnO. This difference in the band gap was due to the difference in crystal shape and size of the nondoped and doped ZnO samples [18] [20].

3.5. Photocatalytic Activity for Degradation of Methylene Blue Dye

Figure 6 was the plot to study the photocatalytic activity of ZnO samples for the degradation of methylene blue (MB) under UV irradiation.

The plots in **Figure 6** showed that the 2%Cu-ZnO sample was the most for degradation of the MB dye solution, and achieved the decomposition efficiency of about 97%; the 5%Cu-ZnO sample achieved the decomposition efficiency of about 96%; the 7%Cu-ZnO sample had a decomposition efficiency of about 92.6% and the ZnO pure sample had the lowest decomposition efficiency of about 20%. It could be seen that the different content of Cu dopant into the pure ZnO lattice changed the shape and size of the crystal particles of the prepared

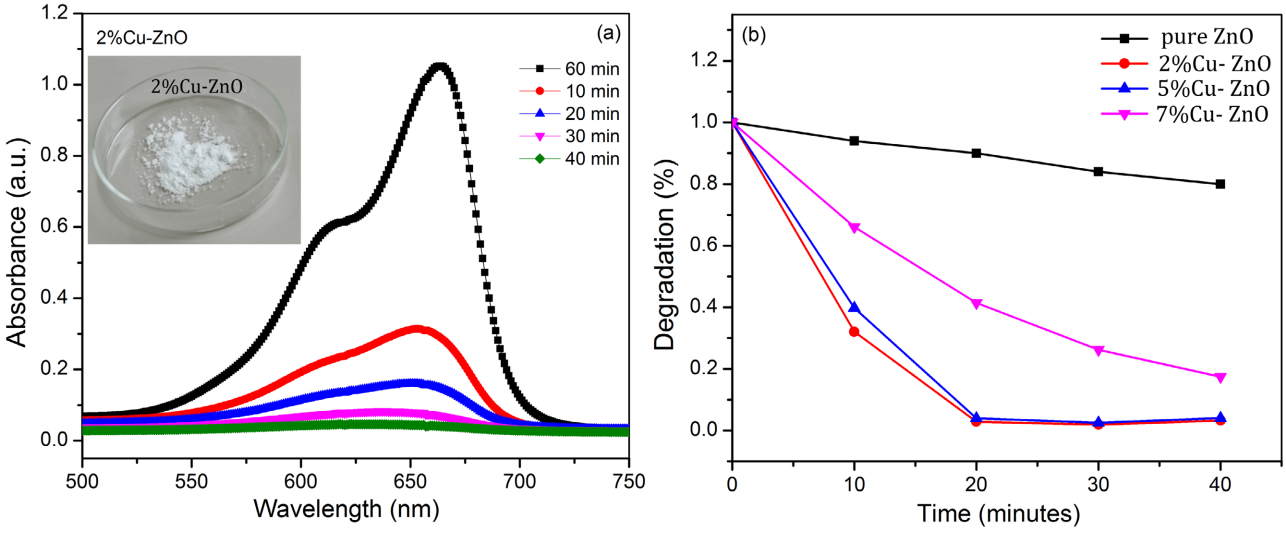

Figure 6. (a) The plot of absorbance versus reaction time. Inset: Photographs of 2%Cu-ZnO nanorods samples of the experiment. (b) The plot of the decrease in MB dye concentration against the reaction time of the pure ZnO and Cu^{2+} doped ZnO samples.

samples and led to an improvement in the photocatalytic performance for degradation of MB dye solution. The highest MB degradation efficiency was obtained in the ZnO sample with a copper doping concentration of 2 mol.%.

4. Conclusion

This study had been successfully synthesized by hydrothermal method for pure ZnO and Cu-doped ZnO nanorods samples with the change of dopant content at 2, 5 and 7 mol.%. The properties of the material samples were investigated, such as XRD method, Raman shift spectra, SEM, and Kubelka-Munk model analysis (K-M) based on the DRS reflectance spectrum. XRD and Raman spectra showed the material samples all have the wurtzite hexagonal structure of ZnO with space group (P63mc). The average crystal size of the Cu-doped samples was more reduced (reached 22.6 - 20.4 nm) than that of pure ZnO (64.5 nm). The pure ZnO and Cu-doped ZnO samples both had a shape in rods with the rods size decreasing and the rods porosity increasing when Cu doped into the ZnO lattice (reached of about 250 - 300 nm for pure ZnO sample; 20 - 30 nm for 2%Cu-ZnO sample; 100 - 200 nm for 5%Cu-ZnO and 7%Cu-ZnO samples). The band gap of the prepared samples based on the K-M model was determined to be 3.31 eV, 3.17 eV, 3.16 eV and 3.15 eV for the pure ZnO, 2%Cu-ZnO, 5%Cu-ZnO and 7%Cu-ZnO samples, respectively. Evaluation of photocatalytic activity showed that the degradation efficiency for MB dye solution was highest at 2%Cu-ZnO sample, reached about 97%, and the lowest decomposition efficiency was the pure ZnO sample, reached about 20%.

Acknowledgements

This work was funded by Hanoi University of Science and Technology (HUST) under the project number T2018-PC-233. This work was funded by Hanoi Uni-

versity of Science and Technology (HUST) under the project number AGF.2022-04. And the authors also thank for the support by the Hanoi University of Science and Technology (HUST) under the project number CT2022.04.BKA.05, Science and Technology Project of the Ministry of Education and Training of Vietnam.

Conflicts of Interest

The authors declare no conflicts of interest regarding the publication of this paper.

References

[1] Mote, V.D., Purushotham, Y. and Dole, B.N. (2012) Williamson-Hall Analysis in Estimation of Lattice Strain in Nanometer-Sized ZnO Particles. *Theoretical and Applied Physics*, **6**, Article No. 6. http://www.jtaphys.com/content/2251-7235/6/1/6 https://doi.org/10.1186/2251-7235-6-6

[2] Gupta, T.K. (1990) Application of Zinc Oxide Varistors. *Journal of the American Ceramic Society*, **73**, 1817-1840. https://doi.org/10.1111/j.1151-2916.1990.tb05232.x

[3] Fangli, Y., Shulan, H. and Jinlin, L. (2001) Preparation of Zinc Oxide Nano-Particles Coated with Aluminum. *Journal of Materials Science Letters*, **20**, 1549-1551. https://doi.org/10.1023/A:1017959404481

[4] Iwasaki, M., Inubushi, Y. and Ito, S. (1997) New Route to Prepare Ultrafine ZnO Particles and Its Reaction Mechanism. *Journal of Materials Science Letters*, **16**, 1503-1505. https://doi.org/10.1023/A:1018566923329

[5] Vayssieres, L. (2003) Growth of Arrayed Nanorods and Nanowires of ZnO from Aqueous Solutions. *Advanced Materials*, **15**, 464-466. https://doi.org/10.1002/adma.200390108

[6] Xu, S. and Wang, Z.L. (2011) One-Dimensional ZnO Nanostructures: Solution Growth and Functional Properties. *Nano Research*, **4**, 1013-1098. https://doi.org/10.1007/s12274-011-0160-7

[7] Look, D. (2001) Recent Advances in ZnO Materials and Devices. *Materials Science and Engineering*: *B*, **80**, 383-387. https://doi.org/10.1016/S0921-5107(00)00604-8

[8] Yi, G.C., Wang, C. and Il Park, W. (2005) ZnO Nanorods: Synthesis, Characterization and Applications. *Semiconductor Science and Technology*, **20**, 22-34. https://doi.org/10.1088/0268-1242/20/4/003

[9] Wang, Z.L. (2004) Zinc Oxide Nanostructures: Growth, Properties and Applications. *Journal of Physics: Condensed Matter*, **16**, R829-R858. https://doi.org/10.1088/0953-8984/16/25/R01

[10] Wang, B., *et al.* (2009) Effects of Cr-Doping on the Photoluminescence and Ferromagnetism at Room Temperature in ZnO Nanomaterials Prepared by Soft Chemistry Route. *Materials Chemistry and Physics*, **113**, 103-106. https://doi.org/10.1016/j.matchemphys.2008.07.031

[11] Gomez, L. and Tigli, O. (2013) Zinc Oxide Nanostructures: From Growth to Application. *Journal of Materials Science*, **48**, 612-624. https://doi.org/10.1007/s10853-012-6938-5

[12] Alireza, R. and Nader, M. (2017) Post Treatment of Composting Leachate Using ZnO Nanoparticles Immobilized on Moving Media. *Applied Catalysis B*: *Environmental*, **220**, 211-221. https://doi.org/10.1016/j.apcatb.2017.08.042

[13] Silambarasan, M., Saravanan, S. and Soga, T. (2015) Raman and Photoluminescence

Studies of Ag and Fe-doped ZnO Nanoparticles. *International Journal of ChemTech Research*, **7**, 1644-1650.

[14] Mende, L.S. and Driscoll, J.L.M. (2007) ZnO—Nanostructures, Defects and Devices. *Materials Today*, **10**, 40-48. https://doi.org/10.1016/S1369-7021(07)70078-0

[15] Singhal, S., Kaur, J., Namgyal, T. and Sharma, R. (2012) Cu-Doped ZnO Nanoparticles: Synthesis, Structural and Electrical Properties. *Physica B: Condensed Matter*, **407**, 1223-1226. https://doi.org/10.1016/j.physb.2012.01.103

[16] Godini, K., *et al.* (2020) Application of ZnO Nanorods Doped with Cu for Enhanced Sonocatalytic Removal of Cr(VI) from Aqueous Solutions. *Environmental Science and Pollution Research*, **27**, 2691-2706. https://doi.org/10.1007/s11356-019-07165-9

[17] Richa, B., Amardeep, B., Jitendra, P.S., Keun, H.C., Navdeep, G. and Sanjeev, G. (2018) Structural and Electronic Investigation of ZnO Nanostructures Synthesized under Different Environments, *Heliyon*, **4**, E00594. https://doi.org/10.1016/j.heliyon.2018.e00594

[18] Thilagavathi, T. and Geetha, D. (2014) Nano ZnO Structures Synthesized in Presence of Anionic and Cationic Surfactant under Hydrothermal Process. *Applied Nanoscience*, **4**, 127-132. https://doi.org/10.1007/s13204-012-0183-8

[19] Jyacine, C., Ahcène, C., Yannick, L., Mohammed, R., Abdelaziz, K. and Christian, C. (2016) Electrical, Dielectric and Photocatalytic Properties of Fe-Doped ZnO Nanomaterials Synthesized by Sol Gel Method, *Processing and Application of Ceramics*, **10**, 125-135. https://doi.org/10.2298/PAC1603125C

[20] Geetha, D. and Thilagavathi, T. (2010) Hydrothermal Synthesis of Nano ZnO Structures from CTAB. *Journal of Nanomaterials and Biostructures*, **5**, 297-301.

[21] Gu, P., Wang, X., Li, T. and Meng, H. (2012) Synthesis, Characterization and Photoluminescence of ZnO Spindles by Polyvinylpyrrolidone-Assisted Low-Temperature Wet-Chemistry Process. *Journal of Crystal Growth*, **338**, 162-165. https://doi.org/10.1016/j.jcrysgro.2011.10.028

[22] Hong-xia, L., Yun-long, Z., Xiu, J.Y. and Deliang, C. (2011) Controllable Synthesis of Spindle-Like ZnO Nanostructures by a Simple Low-Temperature Aqueous Solution Route. *Applied Surface Science*, **257**, 4519-4523. https://doi.org/10.1016/j.apsusc.2010.12.115

[23] Li, P., Liu, H., Fang-xiang, X. and Wei, Y. (2008) Controllable Growth of ZnO Nanowhiskers by a Simple Solution Route. *Materials Chemistry and Physics*, **112**, 393-397. https://doi.org/10.1016/j.matchemphys.2008.05.065

[24] Chu, S.-Y., Yan, T.M. and Chen, S.L. (2000) Characteristics of Sol-Gel Synthesis of ZnO-Based Powders. *Journal of Materials Science Letters*, **19**, 349-352.

[25] Suwanboon, S. (2008) Structural and Optical Properties of Nanocrystalline ZnO Powder from Sol-Gel Method. *ScienceAsia*, **34**, 31-34. https://doi.org/10.2306/scienceasia1513-1874.2008.34.031

[26] Usui, H. (2009) The Effect of Surfactants on the morphology and Optical Properties of Precipitated Wurtzite ZnO. *Materials Letters*, **63**, 1489-1492. https://doi.org/10.1016/j.matlet.2009.03.054

[27] Radha, B., *et al.* (2018) Effect of Fe Doping on the Photocatalytic Activity of ZnO Nanoparticles: Experimental and Theoretical Investigations. *Journal of Materials Science: Materials in Electronics*, **29**, 13474-13482. https://doi.org/10.1007/s10854-018-9472-7

[28] Wibowo, J.A., *et al.* (2013) Cu- and Ni-Doping Effect on Structure and Magnetic Properties of Fe-Doped ZnO Nanoparticles. *Advances in Materials Physics and Che-*

mistry, **3**, 48-57. https://doi.org/10.4236/ampc.2013.31008

[29] Dhiman, P., *et al.* (2012) Structural and Electrical Properties of Fe Doped ZnO Nanoparticles Synthesized by Solution Combustion Method. *Solid State Physics*, **1447**, 307-308. https://doi.org/10.1063/1.4710002

[30] Bhardwaj, R., Bharti, A., Singh, J.P., Chae, K.H., Goyal, N. and Gautam, S. (2018) Structural and Electronic Investigation of ZnO Nanostructures Synthesized under Different Environments. *Heliyon*, **4**, e00594. https://doi.org/10.1016/j.heliyon.2018.e00594

[31] Zeferino, R.S., Flores, M.B. and Pal, U. (2011) Photoluminescence and Raman Scattering in Ag-Doped ZnO Nanoparticles. *Journal of Applied Physics*, **109**, Article ID: 014308. https://doi.org/10.1063/1.3530631

[32] Pal, B. and Giri, P.K. (2011) Defect Mediated Magnetic Interaction and High Tc Ferromagnetism in Co Doped ZnO Nanoparticles. *Journal of Nanoscience and Nanotechnology*, **11**, 9167-9174. https://doi.org/10.1166/jnn.2011.4293

[33] Wang, Y., Ma, Q., Jia, H. and Wang, Z. (2016) One-Step Solution Synthesis and Formation Mechanism of Flower-Like ZnO and Its Structural and Optical Characterization. *Ceramics International*, **42**, 10751-10757. https://doi.org/10.1016/j.ceramint.2016.03.200

[34] Gnanaprakasam, A., Sivakumar V.M. and Thirumarimurugan, M. (2016) A Study on Cu and Ag Doped ZnO Nanoparticles for the Photocatalytic Degradation of Brilliant Green Dye: Synthesis and Characterization. *Water Science & Technology*, **74**, 1426-1435. https://doi.org/10.2166/wst.2016.275

[35] Amin, G., Asif, M.H., Zainelabdin, A., Zaman, S., Nur, O. and Willander, M. (2011) Influence of pH, Precursor Concentration, Growth Time and Temperature on the Morphology of ZnO Nanostructures Grown by the Hydrothermal Method. *Journal of Nanomaterials*, **2011**, Article ID: 269692. https://doi.org/10.1155/2011/269692